OUT-OF-PLANE DISPLACEMENT ANALYSIS USING PANORAMIC ELECTRONIC SPECKLE PATTERN INTERFEROMETRY

Sara B. Fair
Consortium for Holography, Applied Mech. & Photonics
University of Alabama in Huntsville
Huntsville, Alabama 35899

John A. Gilbert
Department of Mechanical and Aerospace Engineering
University of Alabama in Huntsville
Huntsville, Alabama 35899

Donald R. Matthys
Physics Department
Marquette University
Milwaukee, Wisconsin 53233

ABSTRACT

This paper describes a panoramic electronic speckle pattern interferometry (ESPI) system that relies on two collinear panoramic annular lenses (PALs), one to illuminate and the other to image the entire circumference of a section of pipe. The governing equation relating the change in phase to the displacements is derived based on modulations in the sensitivity vector over the field of view. Phase stepping is performed using a piezotranslator. The images are acquired with a CCD camera and stored using a frame grabber. Customized software is employed to map the PAL image into a conventional format. Finally, the intensity distribution is analyzed with customized fringe analysis routines: filtering is performed with the addition of digital carrier fringes to remove noise, and phase unwrapping is used to obtain the phase map and the associated displacements.

INTRODUCTION

Conventional electronic speckle pattern interferometry (ESPI) systems are restricted to making displacement measurements on surfaces that are flat or have some minimal curvature associated with them. This restriction is a result of using conventional optics in the experimental setup, such as a collimated or slightly diverging illuminating beam and a forward viewing lens. However, prior research has demonstrated that panoramic annular lenses (PALs) can be used to record holographic interferograms on the interior surfaces of cylinders [1,2,3]. This paper shows how the interferometric capabilities of the PAL can be extended by using the relatively low resolution technique of ESPI.

PANORAMIC ANNULAR LENS

The PAL is a single element lens composed of three spherical surfaces, two convex and one concave, and one flat surface. Non adjacent concave and convex surfaces are mirrored, while the flat and the remaining convex surface are not. As illustrated in Fig. 1, the surfaces are uniquely designed to focus and translate the incoming light (from, *e.g.*, points A and B) in much the same way as a series of lenses and mirrors. They form an internal virtual image (A' and B') which can be transferred by a standard lens to a CCD camera to form a real image (A" and B"). The annular image contains the objects that surround the PAL.

The longitudinal axis, Z, coincides with the optical axis of the lens and a right-handed Cartesian coordinate system is established at the physical center of the PAL where the diameter is the largest. Points A and B, located at the edges of the field of view on a section of pipe surrounding the lens, can be defined with respect to the origin by the angles α_u and α_l, respectively. All points on the cylinder wall contained in the plane defined by z = A are imaged around the inner radius, r_i, of the image annulus. Similarly, points on the cylinder in the plane z = B are imaged around the outer radius, r_o. A linearization algorithm can be used to remove the radial and tangential distortions of the annular image [4].

THE PANORAMIC ESPI SYSTEM

Experiments were performed using the panoramic ESPI system illustrated in Fig. 2. The system was mounted on a vibration isolated table; a krypton laser (λ = 647.1 nm) was used as the coherent light source.

A circular PVC pipe with an inner radius of 50.8 mm (2 in.), a wall thickness of 6.35 mm (0.25 in.), and a length of 101.6 mm (4 in.) was positioned so that its longitudinal axis was coincident with the Z-axis of the dual PAL system. The pipe was positioned in a pneumatic load frame mounted on two kinematic stages having a total of three degrees of freedom in the x, y, and z directions. The precision translation stage was incorporated to facilitate off-axis measurements and to assist in aligning the pipe. A small air cylinder was used to apply diametrical compression over the length of the pipe through a beam fixed to the piston of the air cylinder.

The two PALs were centered along the length of the pipe and spaced at a distance of 27 mm (1.06 in.) apart. A spatial filter was used to expand the object beam entering the illuminating PAL, and a 20 mm (0.787 in.) diameter, 0.762 mm (0.03 in.) thick, stop was centered and fixed to

the front of this lens to block stray light from entering the imaging system. The virtual image of the pipe formed by the viewing PAL was transferred to the detector of a Pulnix CCD camera using a 105-mm (4.13 in.) Nikon lens. An *f*/11 aperture was used to provide optimum fringe contrast.

The reference beam was split from the object beam using the variable density attenuator labeled as VA_1. A second attenuator, VA_2, was used to control the intensity of a speckle pattern formed by placing a ground glass plate in the reference beam at the same distance from the camera as the test surface. A mask with an open aperture equal to the size of the annular image produced by the imaging PAL was affixed to the ground glass plate to help reduce noise in the image plane.

A low voltage piezotranslator (PZT) was used to obtain a phase change in the reference beam required for phase stepping. The PZT assembly was mounted behind the mirror labeled as M_2. The total voltage required to produce a 2π phase shift was calibrated, and a voltage divider was designed to produce input voltages to the PZT corresponding to 0, 25, 50, 75, and 100% of the total phase shift.

GOVERNING EQUATION AND SENSITIVITY VECTOR

Figure 3 shows two PALs spaced at a distance, dZ, apart. The illuminating PAL produces a circumferential belt on the inner wall of the pipe while the imaging PAL captures a portion of the illuminated surface. Interference is observed over the region of interest (ROI) where the beams overlap.

The phase changes that take place in the ROI are related to the displacement of the surface by the well known equation,

$$\Delta\phi = \frac{2\pi}{\lambda}(e_i - e_v)\cdot d = \frac{2\pi}{\lambda} C_i\, d_i \qquad i = 1,2,3 \qquad (1)$$

where $\Delta\phi$ is the phase change associated with the displacement of a given point. The vectors $\mathbf{e}_i$ and $\mathbf{e}_v$ are unit vectors in the directions of illumination and observation, respectively; and, $\mathbf{C} = (\mathbf{e}_i - \mathbf{e}_v)$ is the sensitivity vector along which the displacement vector $\mathbf{d}$ is projected. The sensitivity vector lies in the plane formed by the illumination and observation vectors, and is directed along their angle bisector. The changes in sensitivity across the ROI of the panoramic ESPI system can be determined by studying the optical characteristics of the lenses.

Figure 4, for example, depicts characteristics determined by combining physical measurements with a ray trace. The entrance pupil of the PAL is offset a distance of z = 6.7 mm (0.26 in.) toward the front of the lens, and y = 1.3 mm (0.05 in.) from the origin. The angular field of view, measured from this point, is 45.4°. The latter determines the maximum size of the region that can be illuminated or imaged by the lens and extends over the range $-18.8° \le \phi_i \le 26.6°$, where ϕ_i is the field angle. The field of view covers 41.6 mm (1.64 in.) for a surface located 50.8 mm (2 in.) from the Z axis. The equation describing the direction of propagation of the illuminating or viewing wavefront, given by the angle e_i, in terms of the field angle, ϕ_i, for the i^{th} point is

$$e_i = 1.004\,\phi_i - 0.2978 \ . \qquad (2)$$

When the propagation angles found over the ROI from a ray trace are compared to those generated using Eq. (2), the error is less than ± 1.3 %. Substituting the propagation vectors, defined by Eq. (2), into Eq. (1),

$$\Delta\phi = \frac{2\pi}{\lambda}\left[\begin{Bmatrix}\cos(1.004\phi_t - 0.2978) + \\ \cos(1.004\phi_v - 0.2978)\end{Bmatrix} d\cos\gamma_d + \begin{Bmatrix}\sin(1.004\phi_i - 0.2978) + \\ \sin(1.004\phi_v - 0.2978)\end{Bmatrix} d\sin\gamma_d\right] \qquad (3)$$

where ϕ_i is the illuminating lens' field angle, ϕ_v is the viewing lens' field angle, and γ_d is the angle between the displacement vector and the sensitivity vector. Since the terms d cos γ_d and d sin γ_d represent the radial and longitudinal displacement components, respectively, there is no sensitivity to circumferential displacement, and

$$\Delta\phi = \frac{2\pi}{\lambda}(C_r\, d_r + C_z\, d_z) \ . \qquad (4)$$

Figure 5 shows a plot of the radial sensitivity coefficient, C_r, versus the field angle over the ROI. Since matched viewing and illuminating wavefronts are used, the direction of the sensitivity vector changes in a symmetric fashion about the center of the ROI, and the plot is symmetrical. The data shows that C_r remains fairly constant over the ROI with a magnitude of approximately 2. The deviation from this value is less than 6.5% for the lens spacing, dZ = 27 mm (1.06 in.), used in the panoramic ESPI system.

The longitudinal sensitivity coefficient, C_z, is plotted in Fig. 6. The sensitivity to longitudinal displacement is significant at points located at the edges of the ROI and goes to zero at the center. At points on the edges of the ROI (defined by the field angles of the illuminating PAL, ϕ_{imax} = 26.58° and ϕ_{imin} = -12.79°), the phase change incorporates 67% of the longitudinal displacement component.

DATA ACQUISITION AND PROCESSING SYSTEM

The hardware required for data acquisition and processing in panoramic ESPI is similar to the system requirements necessary for conventional ESPI. Basically a video camera, image processor, and video monitor are utilized. An array processor was employed to facilitate image processing and increase the speed of computations.

Customized software was developed for the ESPI system to: (1) perform data acquisition of the intensity distribution of the combined reference and object beams at the image plane, (2) linearize the annular image into rectangular format so that fringe analysis could be performed, and (3) produce a phase map corresponding to the difference between the unloaded and loaded states. The goal was to calculate displacements from the phase map using Eq. (1).

Figure 7 shows the noisy fringe pattern of the cylinder under compression obtained with the panoramic EPSI system. The image was linearized and filtered. Phase wrapped

images, such as the one shown in Fig. 8, were obtained following the method described by Sciammarella et al. [5].

As expected, fewer fringes were present at the bottom of the pipe than at the top where the load was applied. In addition, the fringe patterns obtained were fairly symmetric about the vertical centerline of the pipe. However, the phases obtained are indeterminate to a factor of 2π because the arctangent is defined over a range of $-\pi$ to π. Thus, the phase distribution is discontinuous over the field of view.

Phase unwrapping was applied to the phase data to produce a continuous, two-dimensional phase distribution. Figure 9 shows a plot of the displacements around the circumference of the pipe at the center of the ROI. A maximum deformation of -1.35 µm (5.3×10^{-6} in.) was found at the top of the pipe (at the 90° position), due to the compressive load applied there.

Figure 10 depicts the cross-sections of the undeformed and exaggerated deformed pipe located at the center of the ROI. Displacements have been scaled so that the maximum displacement at the top of the pipe is 6.35 mm (0.25 in.). The results agree to within a few percent of theory.

REFERENCES

[1] Gilbert, J.A., Matthys, D.R., Hendren, C., "Displacement analysis of the interior walls of a pipe using holo-Interferometry," SPIE Proceedings, Vol. 1554B, 1991, pp. 128-134.

[2] Matthys, D.R., Gilbert, J.A., and Puliparambil, J., "Panoramic holointerferometry," Experimental Mechanics, Vol. 35, 1995, pp. 83-88.

[3] Lindner, J.L., Gilbert, J.A., "Modal analysis using time-average panoramic holo-interferometry," Modal Analysis: The International Journal of Analytical and Experimental Modal Analysis, Vol. 10, 1995, pp. 143-151.

[4] Matthys, D.R., Gilbert, J.A., and Puliparambil, J., "Endoscopic inspection using a panoramic annular lens," SPIE Proceedings, Vol. 1554B, 1991, pp. 1455-1460.

[5] Sciammarella, C.A., Bhat, G., "Computer assisted techniques to evaluate fringe patterns," SPIE Proceedings, Vol. 1554B, 1991, pp. 162-173.

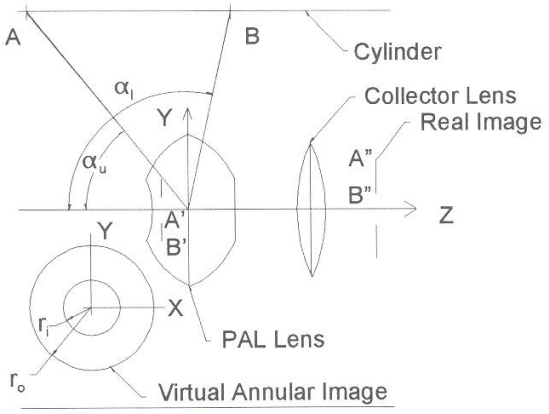

Fig. 1. An annular image is captured by a panoramic annular lens (PAL).

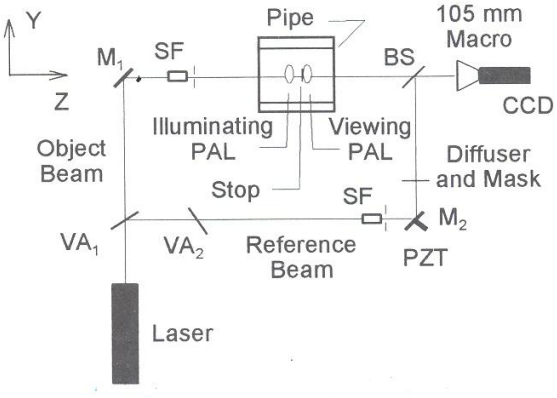

Fig 2. The panoramic ESPI system.

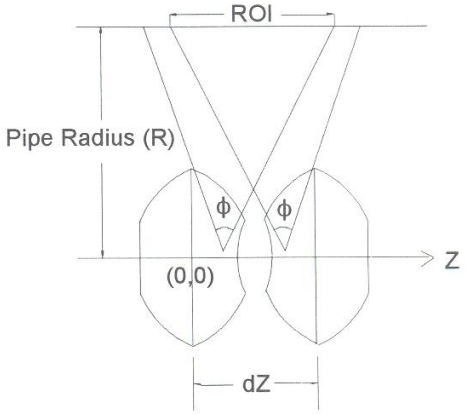

Fig. 3. A dual PAL system.

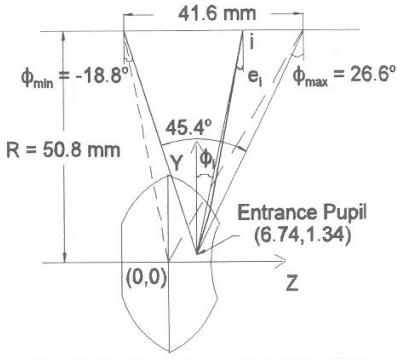

Fig. 4. Optical characteristics of the illuminating PAL.

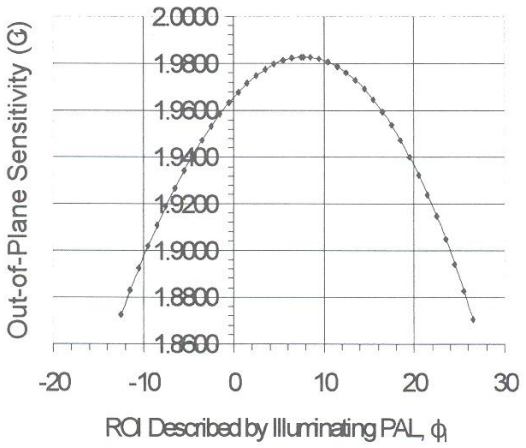

Fig. 5. Radial sensitivity coefficient.

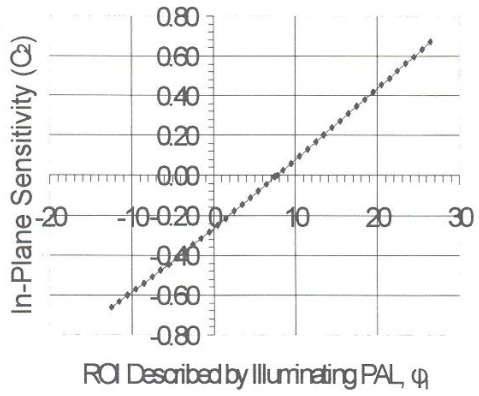

Fig. 6. Longitudinal sensitivity coefficient.

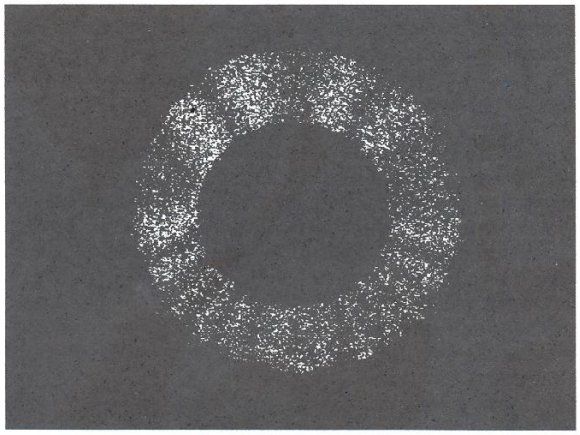

Fig. 7. Noisy fringe pattern prior to filtering.

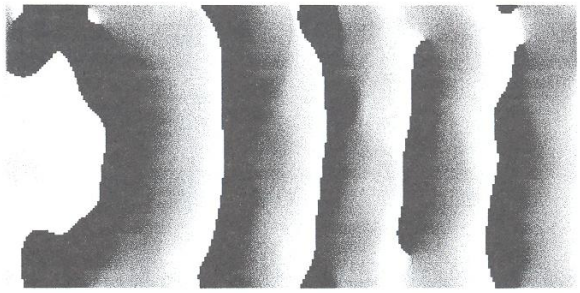

Fig. 8. Phase wrapped image of the fourth quadrant of the image shown in Fig. 7.

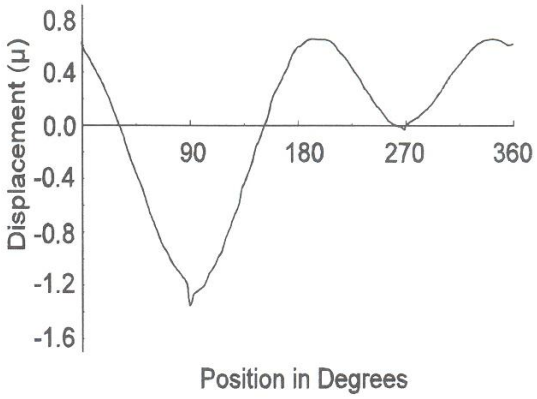

Fig. 9. Radial displacement over the circumference of the pipe at the center of the region of interest ($\phi_i = \phi_v$).

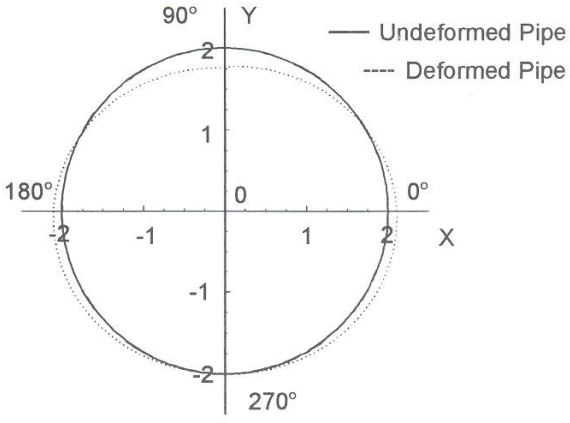

Fig. 10. Scaled deformation of the pipe at the center of the ROI compared to the undeformed cross section.